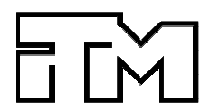


Modeling and Characterization of Continuous-Discontinuous Long Fiber-Reinforced Polymer Structures

Thomas Böhlke (KIT-ITM), Frank Henning (KIT-FAST), Luise Kärger (KIT-FAST),
Thomas Seelig (KIT-IFM), Kay André Weidenmann (KIT-IAM-WK)

14. Deutsches LS-DYNA Forum



University
of Windsor



UNIVERSITY OF
WATERLOO

Western
UNIVERSITY • CANADA

Outline

- Introduction of GRK2078 CoDiCoFRP
 - Motivation and Objectives
- Research Topics
 - Preliminary Remarks on Short Fiber Reinforced Polymers
 - Microscale Characterization
 - Microscale Simulation and Homogenization
 - Macroscale Simulation and Characterization
 - Form Filling Micromechanical Modeling
- Conclusions and Outlook

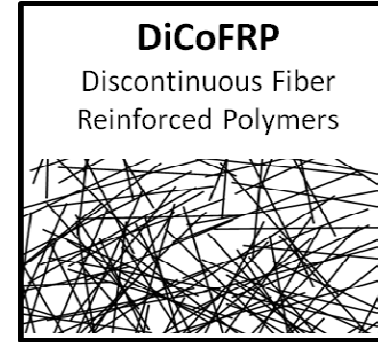
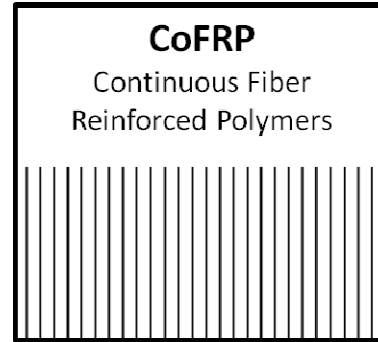
FRP Classes: Introduction and Application

- + High fiber volume content
- + Controlled fibers alignment
- + High stiffness and strength
- Restricted formability
- High cycle times
- High scrap rate
- Extensive trimming



Source: BMW AG Group

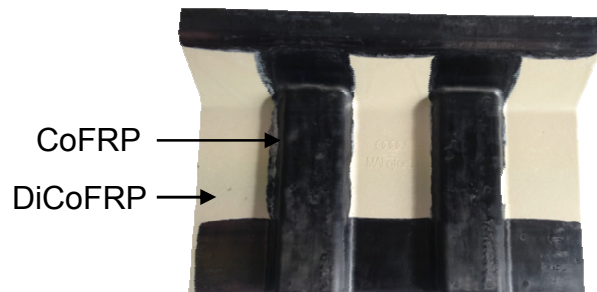
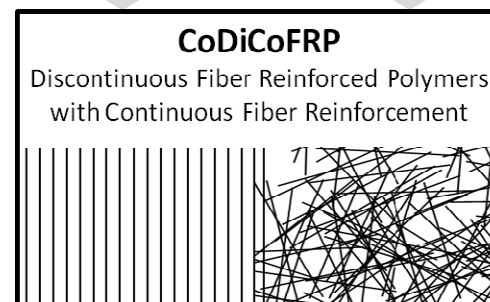
Carbon cell



- + Good formability
- + Function integration potential
- + Low finishing demands
- + Low cycle times
- Low stiffness and strength
- Process related complex microstructure



Frontend made of DiCoFRP

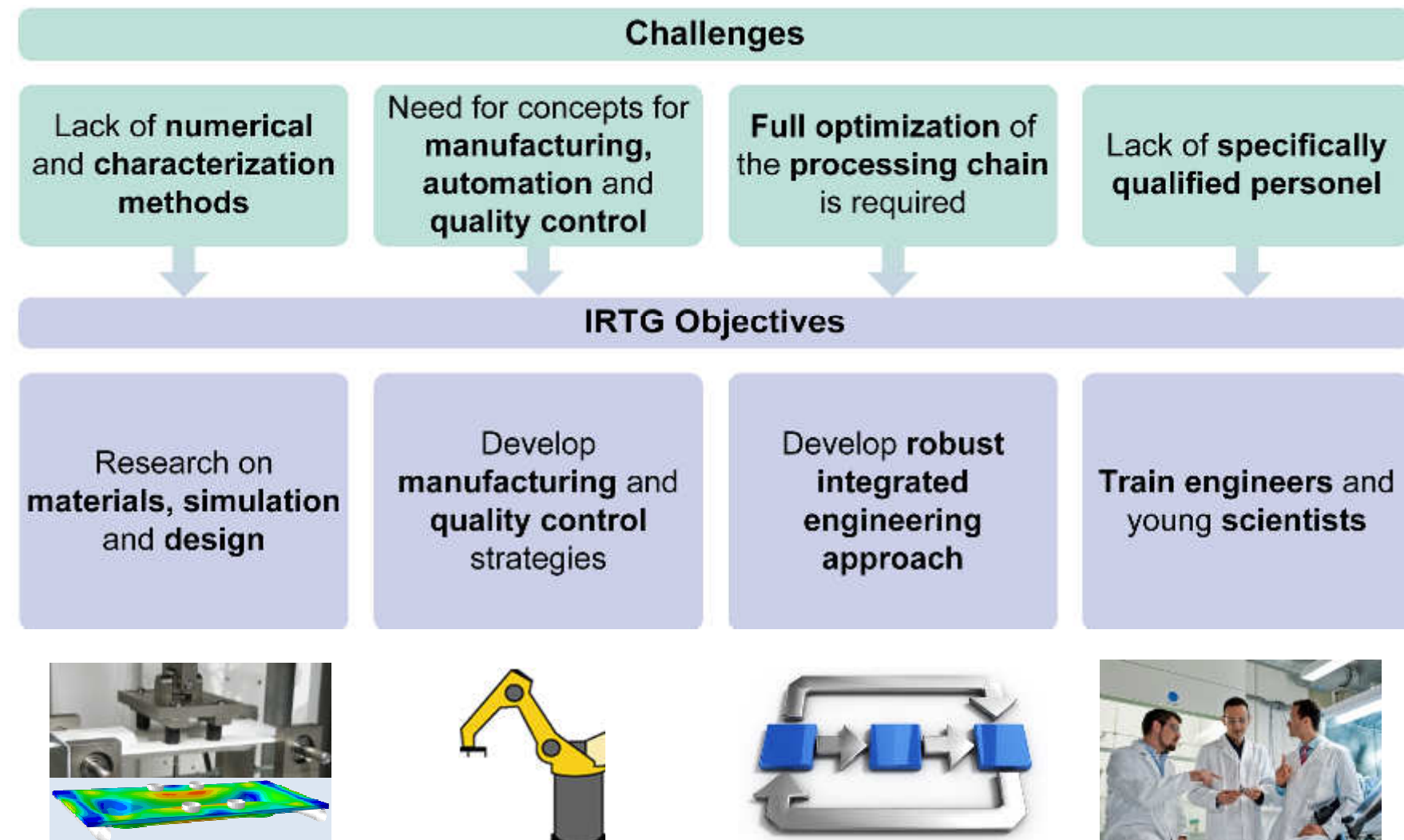


CoDiCoFRP component (front side)

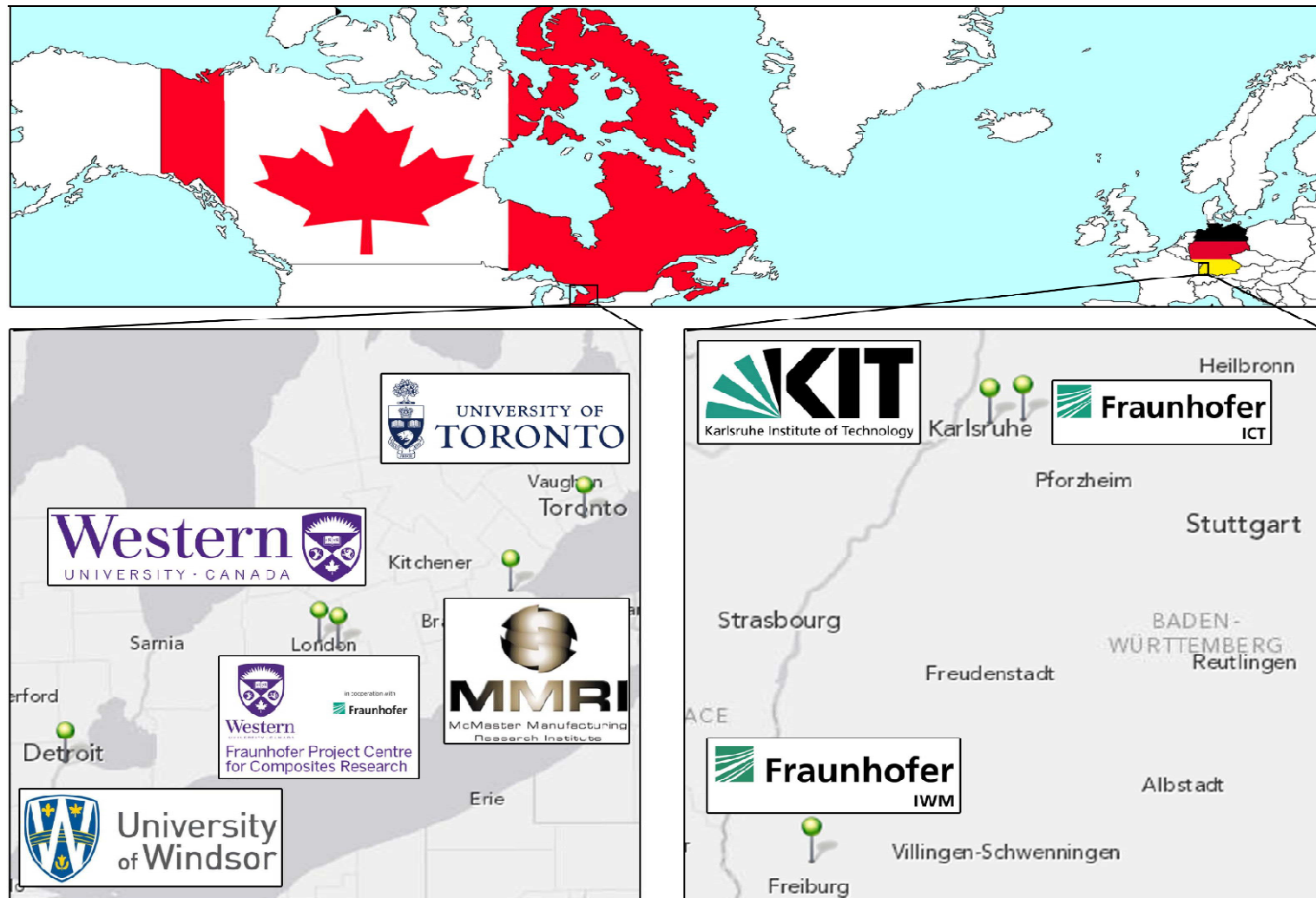


CoDiCoFRP component (back side)

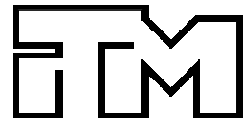
Challenges and Program Objectives



GRK 2078 Twin Regions



DFG GRK2078 Participating Institutes



Thomas Böhlke, Institute of Engineering Mechanics



Fraunhofer
ICT



Peter Elsner, Frank Henning, Fraunhofer-ICT



Albert Albers, Institute of Product Engineering



Peter Gumbsch, Jörg Hohe, Fraunhofer-IWM



Britta Nestler, Kay Weidenmann, Institute for Applied Materials



Luise Kärger, Institute for Vehicle Science



Gisela Lanza, Jürgen Fleischer, Volker Schulze,
Institute of Production Science



Thomas Seelig, Institute of Mechanics

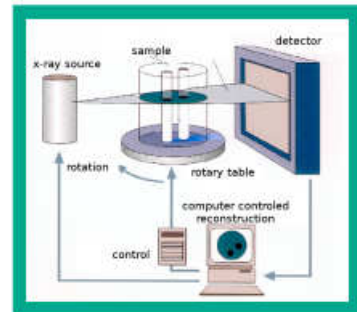


Motivation: Homogenization of Elastic Properties of Short-Fiber Reinforced Composites

Contact: Viktor Müller

μ CT Measurement and Fiber Segmentation

Müller et al. (JCM, 2015), cooperation with Dillenberger, Glöckner, Kolling



μ CT measurement

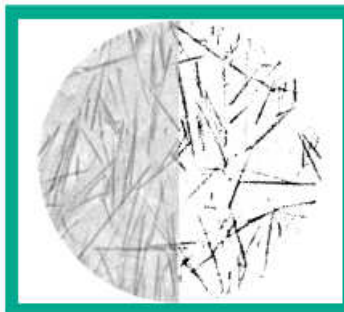
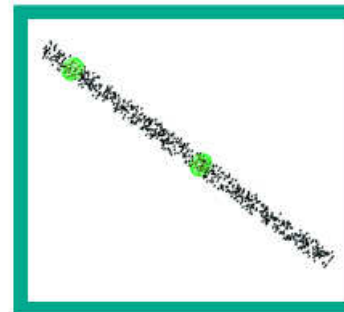


image processing



percolation algorithm

A screenshot of a software application window titled "Voronoi-Mesh - Intersections mit markierten Punkten". The window displays a large grid of numerical data, representing the resulting segmented data from the percolation algorithm.

Line ID	x	y	z
1	1.0000	0.0000	0.0000
2	1.0000	0.0000	0.0000
3	1.0000	0.0000	0.0000
4	1.0000	0.0000	0.0000
5	1.0000	0.0000	0.0000
6	1.0000	0.0000	0.0000
7	1.0000	0.0000	0.0000
8	1.0000	0.0000	0.0000
9	1.0000	0.0000	0.0000
10	1.0000	0.0000	0.0000
11	1.0000	0.0000	0.0000
12	1.0000	0.0000	0.0000
13	1.0000	0.0000	0.0000
14	1.0000	0.0000	0.0000
15	1.0000	0.0000	0.0000
16	1.0000	0.0000	0.0000
17	1.0000	0.0000	0.0000
18	1.0000	0.0000	0.0000
19	1.0000	0.0000	0.0000
20	1.0000	0.0000	0.0000
21	1.0000	0.0000	0.0000
22	1.0000	0.0000	0.0000
23	1.0000	0.0000	0.0000
24	1.0000	0.0000	0.0000
25	1.0000	0.0000	0.0000
26	1.0000	0.0000	0.0000
27	1.0000	0.0000	0.0000
28	1.0000	0.0000	0.0000
29	1.0000	0.0000	0.0000
30	1.0000	0.0000	0.0000
31	1.0000	0.0000	0.0000
32	1.0000	0.0000	0.0000
33	1.0000	0.0000	0.0000
34	1.0000	0.0000	0.0000
35	1.0000	0.0000	0.0000
36	1.0000	0.0000	0.0000
37	1.0000	0.0000	0.0000
38	1.0000	0.0000	0.0000
39	1.0000	0.0000	0.0000
40	1.0000	0.0000	0.0000
41	1.0000	0.0000	0.0000
42	1.0000	0.0000	0.0000
43	1.0000	0.0000	0.0000
44	1.0000	0.0000	0.0000
45	1.0000	0.0000	0.0000
46	1.0000	0.0000	0.0000
47	1.0000	0.0000	0.0000
48	1.0000	0.0000	0.0000
49	1.0000	0.0000	0.0000
50	1.0000	0.0000	0.0000
51	1.0000	0.0000	0.0000
52	1.0000	0.0000	0.0000
53	1.0000	0.0000	0.0000
54	1.0000	0.0000	0.0000
55	1.0000	0.0000	0.0000
56	1.0000	0.0000	0.0000
57	1.0000	0.0000	0.0000
58	1.0000	0.0000	0.0000
59	1.0000	0.0000	0.0000
60	1.0000	0.0000	0.0000
61	1.0000	0.0000	0.0000
62	1.0000	0.0000	0.0000
63	1.0000	0.0000	0.0000
64	1.0000	0.0000	0.0000
65	1.0000	0.0000	0.0000
66	1.0000	0.0000	0.0000
67	1.0000	0.0000	0.0000
68	1.0000	0.0000	0.0000
69	1.0000	0.0000	0.0000
70	1.0000	0.0000	0.0000
71	1.0000	0.0000	0.0000
72	1.0000	0.0000	0.0000
73	1.0000	0.0000	0.0000
74	1.0000	0.0000	0.0000
75	1.0000	0.0000	0.0000
76	1.0000	0.0000	0.0000
77	1.0000	0.0000	0.0000
78	1.0000	0.0000	0.0000
79	1.0000	0.0000	0.0000
80	1.0000	0.0000	0.0000
81	1.0000	0.0000	0.0000
82	1.0000	0.0000	0.0000
83	1.0000	0.0000	0.0000
84	1.0000	0.0000	0.0000
85	1.0000	0.0000	0.0000
86	1.0000	0.0000	0.0000
87	1.0000	0.0000	0.0000
88	1.0000	0.0000	0.0000
89	1.0000	0.0000	0.0000
90	1.0000	0.0000	0.0000
91	1.0000	0.0000	0.0000
92	1.0000	0.0000	0.0000
93	1.0000	0.0000	0.0000
94	1.0000	0.0000	0.0000
95	1.0000	0.0000	0.0000
96	1.0000	0.0000	0.0000
97	1.0000	0.0000	0.0000
98	1.0000	0.0000	0.0000
99	1.0000	0.0000	0.0000
100	1.0000	0.0000	0.0000
101	1.0000	0.0000	0.0000
102	1.0000	0.0000	0.0000
103	1.0000	0.0000	0.0000
104	1.0000	0.0000	0.0000
105	1.0000	0.0000	0.0000
106	1.0000	0.0000	0.0000
107	1.0000	0.0000	0.0000
108	1.0000	0.0000	0.0000
109	1.0000	0.0000	0.0000
110	1.0000	0.0000	0.0000
111	1.0000	0.0000	0.0000
112	1.0000	0.0000	0.0000
113	1.0000	0.0000	0.0000
114	1.0000	0.0000	0.0000
115	1.0000	0.0000	0.0000
116	1.0000	0.0000	0.0000
117	1.0000	0.0000	0.0000
118	1.0000	0.0000	0.0000
119	1.0000	0.0000	0.0000
120	1.0000	0.0000	0.0000
121	1.0000	0.0000	0.0000
122	1.0000	0.0000	0.0000
123	1.0000	0.0000	0.0000
124	1.0000	0.0000	0.0000
125	1.0000	0.0000	0.0000
126	1.0000	0.0000	0.0000
127	1.0000	0.0000	0.0000
128	1.0000	0.0000	0.0000
129	1.0000	0.0000	0.0000
130	1.0000	0.0000	0.0000
131	1.0000	0.0000	0.0000
132	1.0000	0.0000	0.0000
133	1.0000	0.0000	0.0000
134	1.0000	0.0000	0.0000
135	1.0000	0.0000	0.0000
136	1.0000	0.0000	0.0000
137	1.0000	0.0000	0.0000
138	1.0000	0.0000	0.0000
139	1.0000	0.0000	0.0000
140	1.0000	0.0000	0.0000
141	1.0000	0.0000	0.0000
142	1.0000	0.0000	0.0000
143	1.0000	0.0000	0.0000
144	1.0000	0.0000	0.0000
145	1.0000	0.0000	0.0000
146	1.0000	0.0000	0.0000
147	1.0000	0.0000	0.0000
148	1.0000	0.0000	0.0000
149	1.0000	0.0000	0.0000
150	1.0000	0.0000	0.0000
151	1.0000	0.0000	0.0000
152	1.0000	0.0000	0.0000
153	1.0000	0.0000	0.0000
154	1.0000	0.0000	0.0000
155	1.0000	0.0000	0.0000
156	1.0000	0.0000	0.0000
157	1.0000	0.0000	0.0000
158	1.0000	0.0000	0.0000
159	1.0000	0.0000	0.0000
160	1.0000	0.0000	0.0000
161	1.0000	0.0000	0.0000
162	1.0000	0.0000	0.0000
163	1.0000	0.0000	0.0000
164	1.0000	0.0000	0.0000
165	1.0000	0.0000	0.0000
166	1.0000	0.0000	0.0000
167	1.0000	0.0000	0.0000
168	1.0000	0.0000	0.0000
169	1.0000	0.0000	0.0000
170	1.0000	0.0000	0.0000
171	1.0000	0.0000	0.0000
172	1.0000	0.0000	0.0000
173	1.0000	0.0000	0.0000
174	1.0000	0.0000	0.0000
175	1.0000	0.0000	0.0000
176	1.0000	0.0000	0.0000
177	1.0000	0.0000	0.0000
178	1.0000	0.0000	0.0000
179	1.0000	0.0000	0.0000
180	1.0000	0.0000	0.0000
181	1.0000	0.0000	0.0000
182	1.0000	0.0000	0.0000
183	1.0000	0.0000	0.0000
184	1.0000	0.0000	0.0000
185	1.0000	0.0000	0.0000
186	1.0000	0.0000	0.0000
187	1.0000	0.0000	0.0000
188	1.0000	0.0000	0.0000
189	1.0000	0.0000	0.0000
190	1.0000	0.0000	0.0000
191	1.0000	0.0000	0.0000
192	1.0000	0.0000	0.0000
193	1.0000	0.0000	0.0000
194	1.0000	0.0000	0.0000
195	1.0000	0.0000	0.0000
196	1.0000	0.0000	0.0000
197	1.0000	0.0000	0.0000
198	1.0000	0.0000	0.0000
199	1.0000	0.0000	0.0000
200	1.0000	0.0000	0.0000
201	1.0000	0.0000	0.0000
202	1.0000	0.0000	0.0000
203	1.0000	0.0000	0.0000
204	1.0000	0.0000	0.0000
205	1.0000	0.0000	0.0000
206	1.0000	0.0000	0.0000
207	1.0000	0.0000	0.0000
208	1.0000	0.0000	0.0000
209	1.0000	0.0000	0.0000
210	1.0000	0.0000	0.0000
211	1.0000	0.0000	0.0000
212	1.0000	0.0000	0.0000
213	1.0000	0.0000	0.0000
214	1.0000	0.0000	0.0000
215	1.0000	0.0000	0.0000
216	1.0000	0.0000	0.0000
217	1.0000	0.0000	0.0000
218	1.0000	0.0000	0.0000
219	1.0000	0.0000	0.0000
220	1.0000	0.0000	0.0000
221	1.0000	0.0000	0.0000
222	1.0000	0.0000	0.0000
223	1.0000	0.0000	0.0000
224	1.0000	0.0000	0.0000
225	1.0000	0.0000	0.0000
226	1.0000	0.0000	0.0000
227	1.0000	0.0000	0.0000
228	1.0000	0.0000	0.0000
229	1.0000	0.0000	0.0000
230	1.0000	0.0000	0.0000
231	1.0000	0.0000	0.0000
232	1.0000	0.0000	0.0000
233	1.0000	0.0000	0.0000
234	1.0000	0.0000	0.0000
235	1.0000	0.0000	0.0000
236	1.0000	0.0000	0.0000

IDD scheme: continuous formulation

Zheng and Du (2001), Du and Zheng (2002), Wu (1997), Müller and TB (IJSS, 2015)

$$\mathbb{C}^{\text{IDD}} = \mathbb{C}_M + \left(\mathbb{I}^s - \sum_{\beta=1}^{N_F} c_\beta \mathbb{M}_\beta \mathbb{P}_\beta^D \right)^{-1} \sum_{\alpha=1}^{N_F} c_\alpha \mathbb{M}_\alpha$$

with $\mathbb{M}_\gamma = (\mathbb{C}_\gamma - \mathbb{C}_M) (\mathbb{I}^s + \mathbb{P}_\gamma (\mathbb{C}_\gamma - \mathbb{C}_M))^{-1}$

Using averaged microstructure description

$$\mathbb{C}^{\text{IDD}} = \mathbb{C}_M + \left(\mathbb{I}^s - c_F \int_S f(\mathbf{n}) \mathbb{M}(\mathbf{n}) \mathbb{P}^D(\mathbf{n}) \, dS \right)^{-1} c_F \int_S f(\mathbf{n}) \mathbb{M}(\mathbf{n}) \, dS$$

with $\mathbb{M}(\mathbf{n}) = (\mathbb{C}_F - \mathbb{C}_M) (\mathbb{I}^s + \mathbb{P}(\mathbf{n}) (\mathbb{C}_F - \mathbb{C}_M))^{-1}$

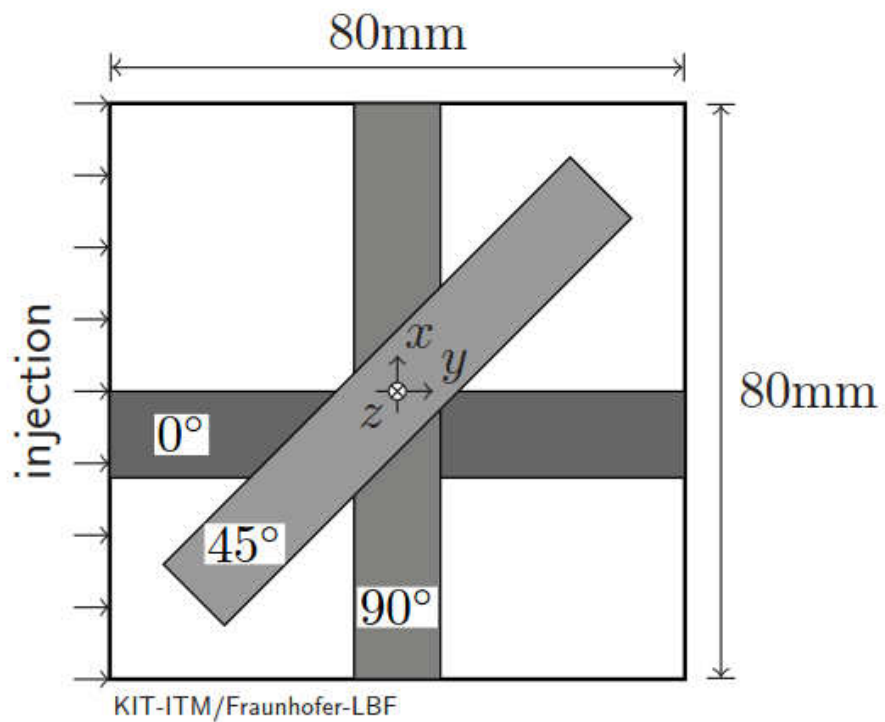
$c_F, f(\mathbf{n})$: total vol. frac. of fibers, FODF

$\mathbb{P}(\mathbf{n}) = \mathbb{P}(\mathbb{C}_M, \mathbb{C}_F, \mathbf{n}, \omega)$: Hill's pol. tensor of fiber with const. aspect ratio

$\mathbb{P}^D(\mathbf{n}) = \mathbb{P}^D(\mathbb{C}_M, \mathbb{C}_F, \mathbf{n}, \omega^D)$: Hill's pol. tensor of cell with const. aspect ratio

Preparation of specimen

Müller et al. (JCM, 2015)

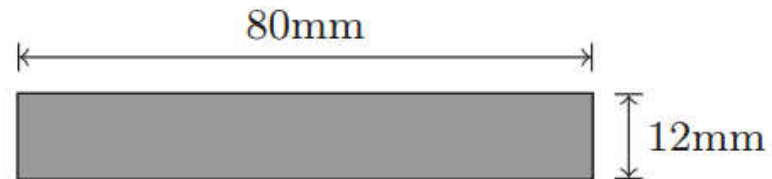


μ CT specimen

Diameter: $d = 2$ mm Height: $h = 2.5$ mm

Position: $P(0, 0)$

Geometry of specimen



Depth: $t = 2.5$ mm

Glass fibers

$E_F = 73.0$ GPa, $\nu_F = 0.22$

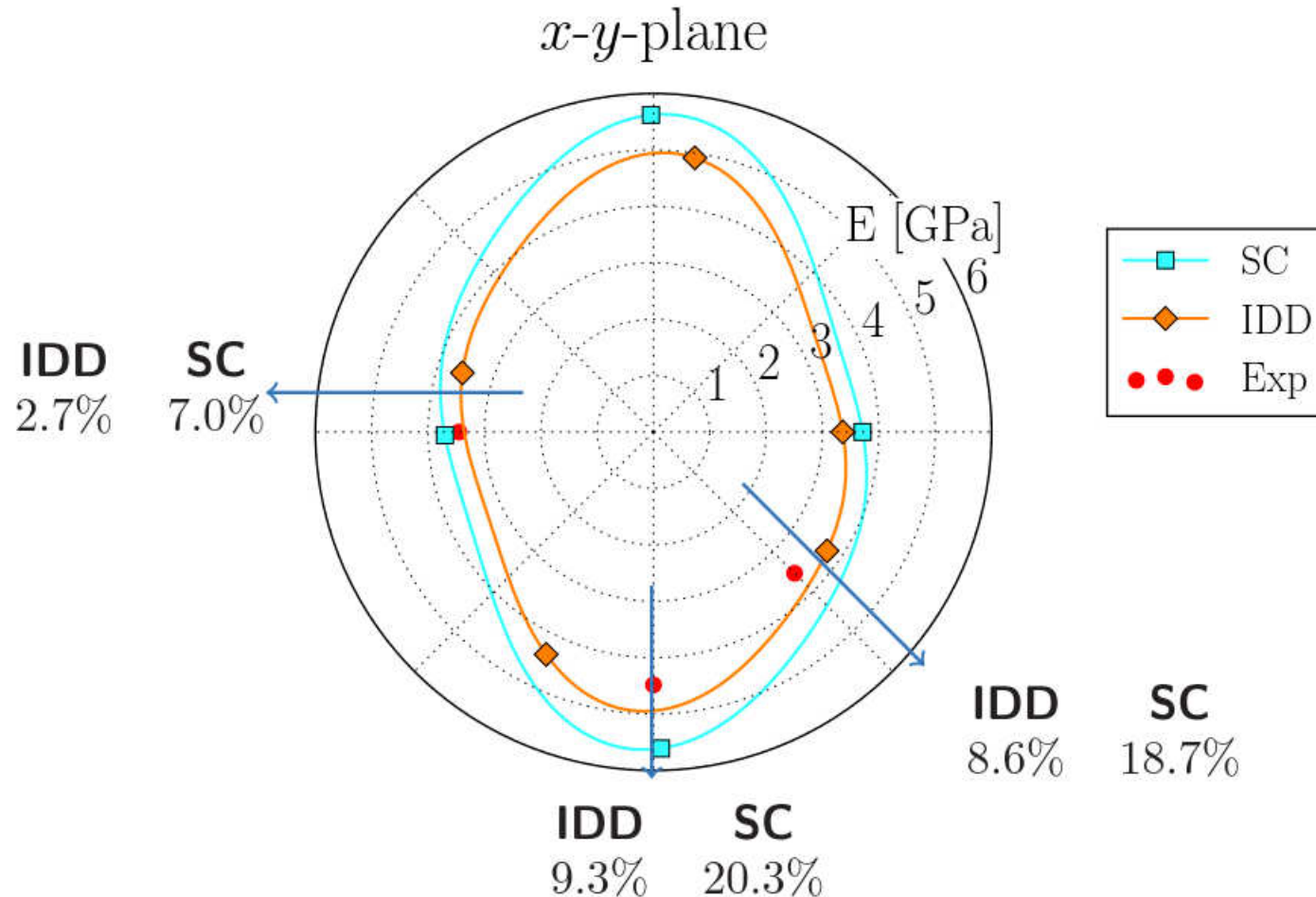
$c_F = 30$ wt.-%

Polypropylene matrix

$E_M = 1.705$ GPa, $\nu_M = 0.355$

Numerical vs experimental results

Müller et al. (JCM, 2015)



Maximum entropy principle (MEP)

Wu (1997), TB (2005), Müller and TB (CSTE, 2015)

First moment problem

$$\bar{\mathcal{S}} := - \int_S \bar{f}(\mathbf{n}) \ln (\bar{f}(\mathbf{n})) \, dS \rightarrow \max$$

$$\mathcal{C}_{<0>} := \int_S \bar{f}(\mathbf{n}) \, dS - 1 \stackrel{!}{=} 0$$

$$\mathcal{C}_{<2>} := \int_S \bar{f}(\mathbf{n})(\mathbf{n} \otimes \mathbf{n})' \, dS - (\mathbf{N})' \stackrel{!}{=} 0$$

$$\mathcal{C}_{<4>} := \int_S \bar{f}(\mathbf{n})(\mathbf{n} \otimes \mathbf{n} \otimes \mathbf{n} \otimes \mathbf{n})' \, dS - (\mathbb{N})' \stackrel{!}{=} 0$$

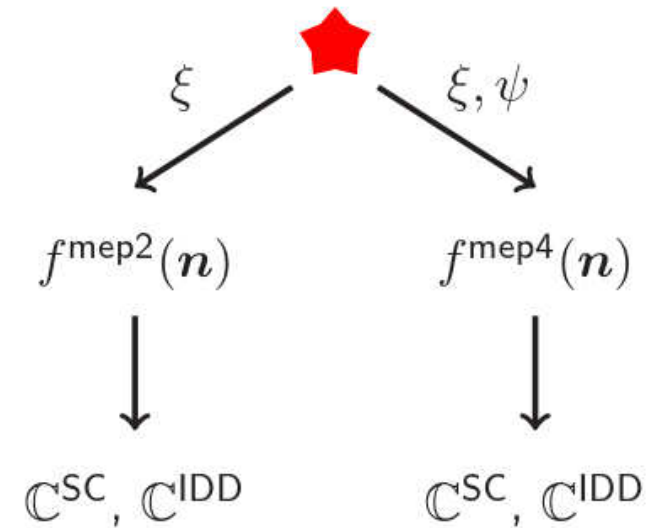
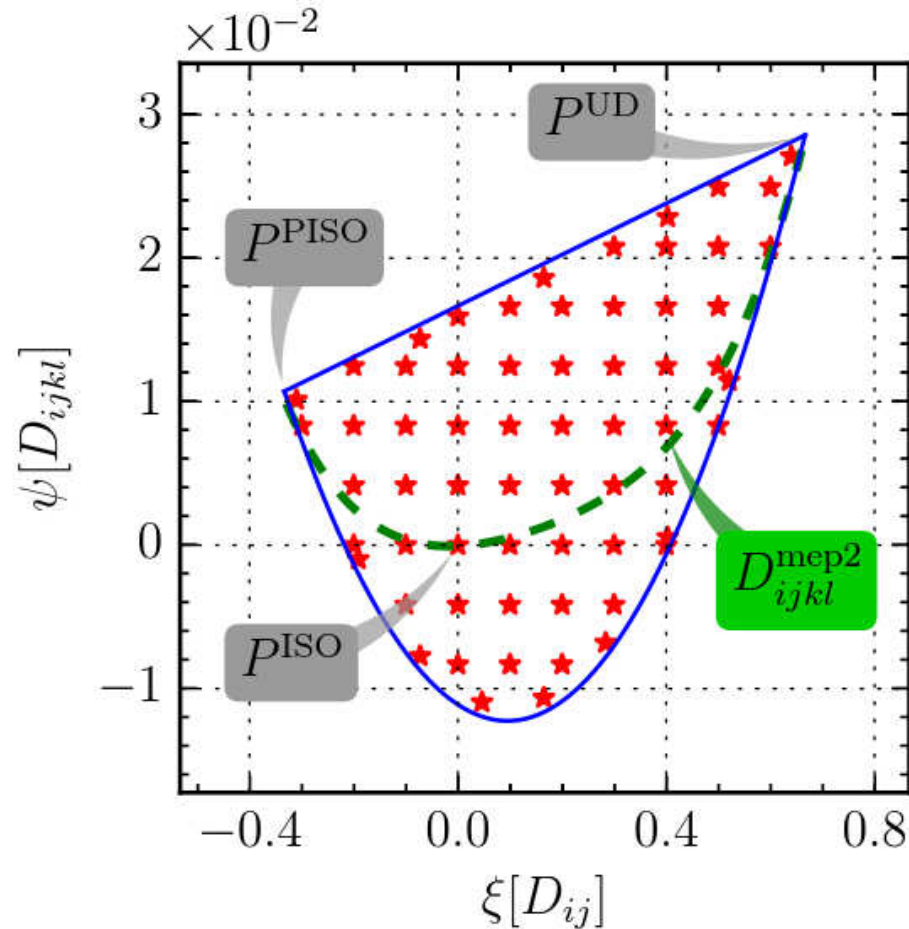
Second moment problem

Optimization with Lagrange multipliers G, G, \mathbb{G}

$$\mathcal{F} = \bar{\mathcal{S}} - G \cdot \mathcal{C}_{<0>} - G \cdot \mathcal{C}_{<2>} - \mathbb{G} \cdot \mathcal{C}_{<4>}$$

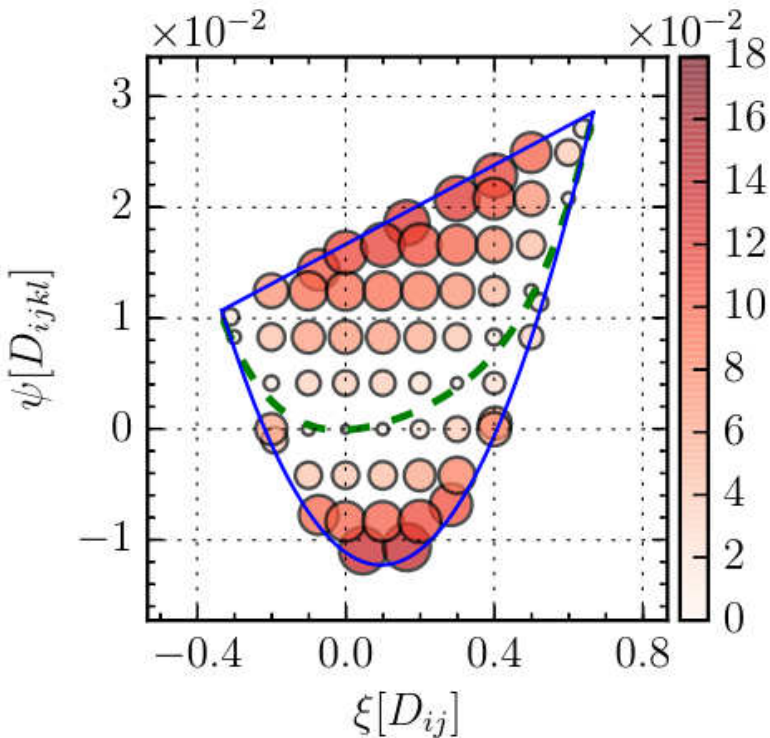
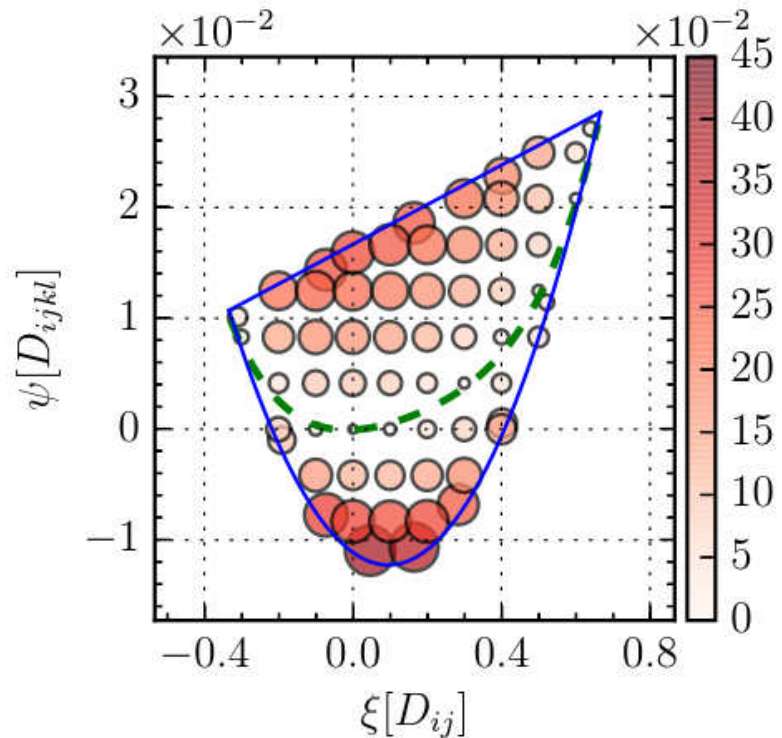
Parameter space for irreducible parameters

Müller and TB (IJSS, 2015)



Deviation of Young's modulus (IDD)

Müller and TB (IJSS, 2015)



$$\frac{\|E_0^{\text{mep4}} - E_0^{\text{mep2}}\|}{\|E_0^{\text{mep4}}\|}$$

$$\frac{\|E_{90}^{\text{mep4}} - E_{90}^{\text{mep2}}\|}{\|E_{90}^{\text{mep4}}\|}$$

Mean Field vs Full-Field Modeling

Material and microstructure parameter

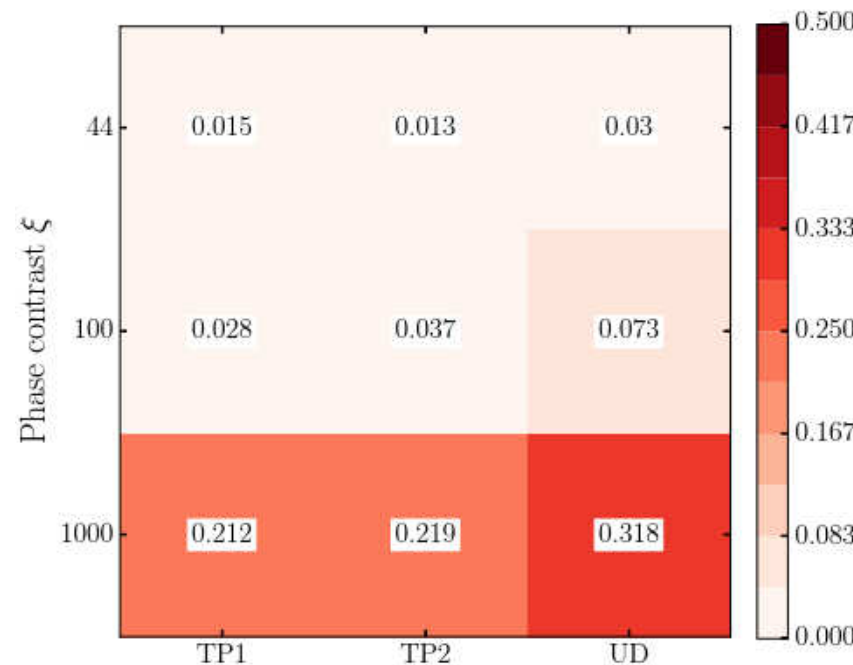
Microstructure	Fiber vol. fraction	UD	Material combination		
			$\eta = 44$	$\eta = 100$	$\eta = 1000$
TP1	TP1/TP2	UD	E_F [GPa]	1.665	1
TP2	13%	13%	ν_F	0.36	0.36
UD		17%	E_M [GPa]	73	100
		12%	ν_M	0.36	0.36

$$\mathbf{N}^{TP1} = \begin{bmatrix} 0.61 & & \\ & 0.36 & \\ & & 0.03 \end{bmatrix} \quad \mathbf{N}^{TP2} = \begin{bmatrix} 0.80 & & \\ & 0.18 & \\ & & 0.02 \end{bmatrix} \quad \mathbf{N}^{UD} = \begin{bmatrix} 1.0 & & \\ & 0.0 & \\ & & 0.0 \end{bmatrix}$$

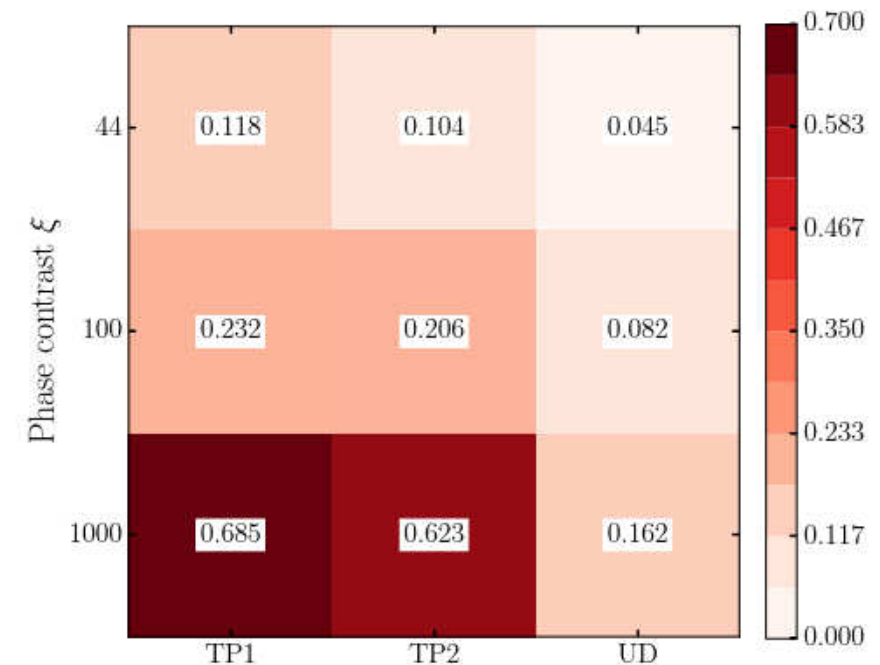
Influence of Phase Contrast and Microstructure

Müller et al. (2015)

MF-IDD vs FFT-BS for $c_F = 13\%$



MF-SC vs FFT-BS for $c_F = 13\%$

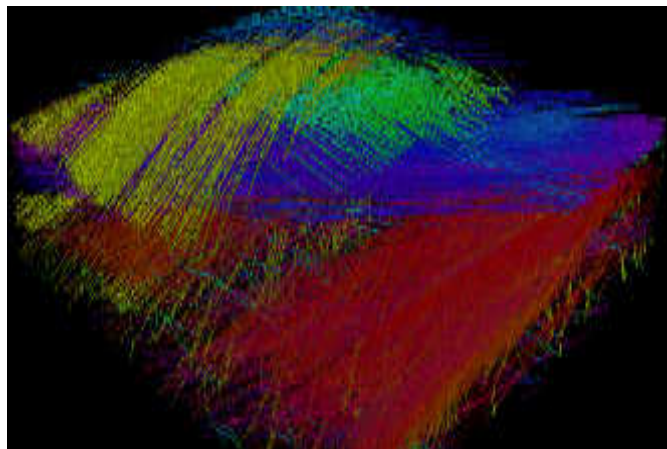


Microscale Characterization

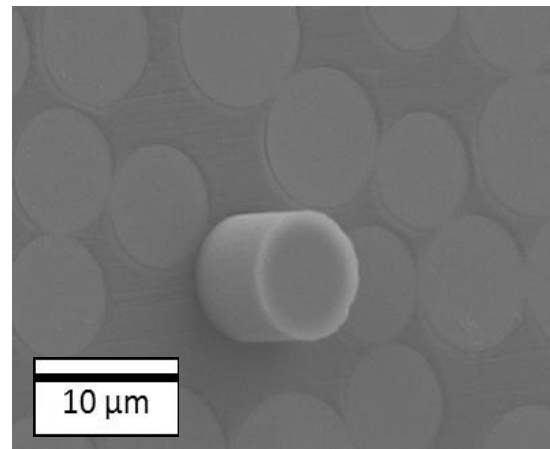
Contact: Pascal Pinter, pascal.pinter@kit.edu, KIT IAM-WK

Microscale Characterization

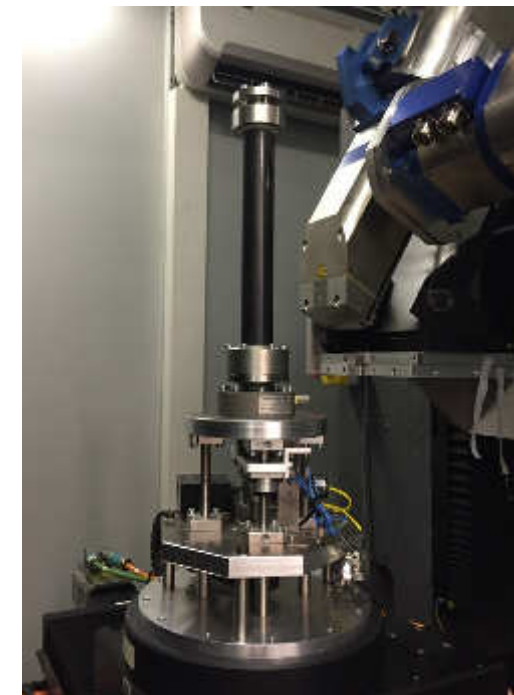
- Development and application of destructive and non-destructive testing methods:
 - Determination of 4th order orientation tensors directly from µCT-scans via in-house software “Composight”
 - Fiber length distributions from µCT-scans
 - Mechanical properties of fibers
 - Interfacial shear strength
 - In-Situ tensile tests for validation of models



Orientation analysis (SMC)



Push-Out-Test



In-Situ-Stage

[Contact: Pascal Pinter, pascal.pinter@kit.edu, KIT IAM-WK]

Microscale Characterization

- Developed methods during IRTG:
 - Fiber orientation distributions: Calculation of 4th order orientation tensors from µCT-Images
 - Fiber length distribution (FLD): Possible specimen size of D=4 mm with 81% correctly traced fibers

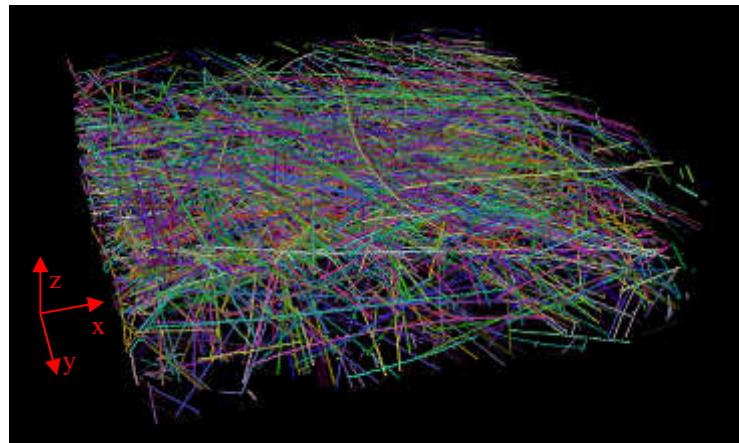
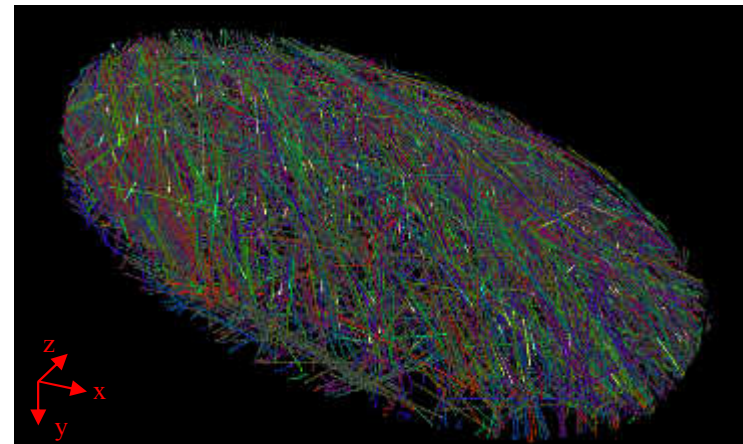
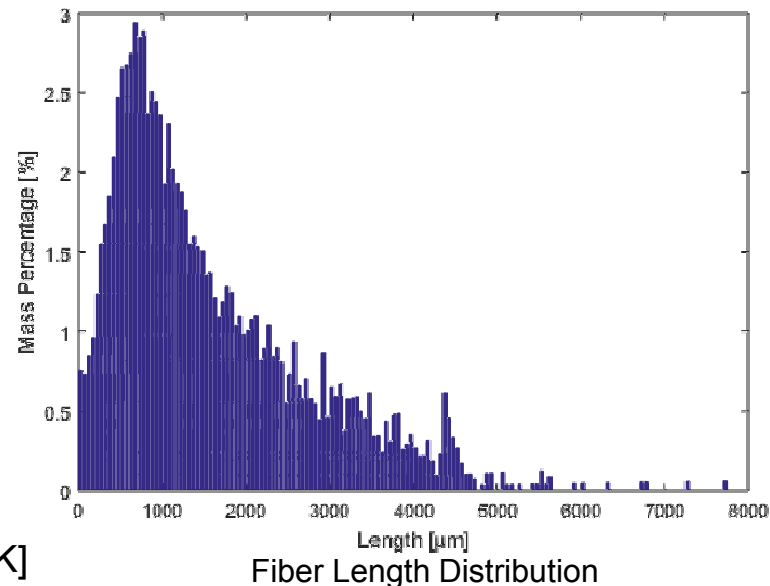


Image detail of same specimen 1.8x1.8x0.5 mm³



LFT20 Ø 4 mm specimen - independent fibers are illustrated in different colors



[Contact: Pascal Pinter, pascal.pinter@kit.edu, KIT IAM-WK]

Microscale Simulation and Homogenization

Contact: Loredana Kehrer, loredana.Kehrer@kit.edu, KIT ITM

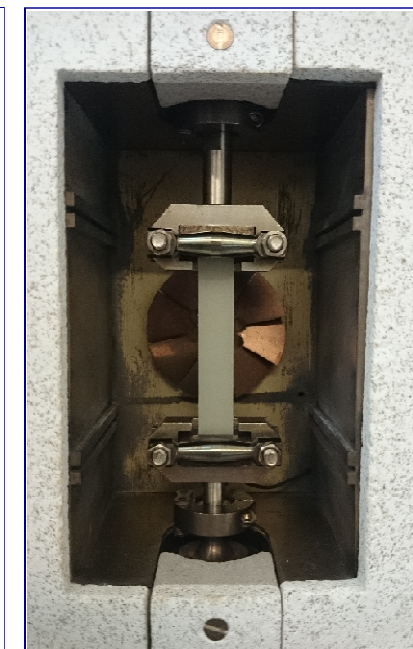
Characterization of mechanical properties by DMA

- Dynamic mechanical analysis (DMA) with GABO Eplexor 500 N
- Analysis of thermal and viscoelastic material properties
- Measured quantities $E^* = E' + iE''$
- Specifications:

Static force	1500 N
Dynamic force	± 500 N
Temperature range	-150°C to 500°C
Frequency range	0.01 Hz to 100 Hz



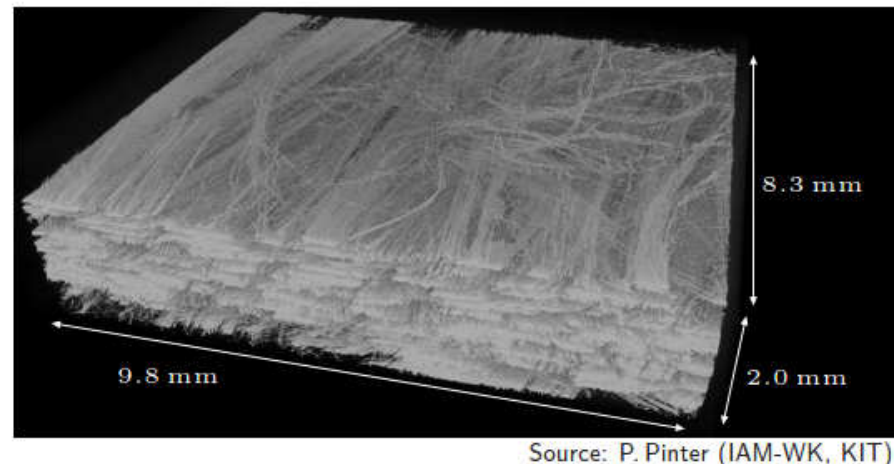
Quelle: GABO



Experimental results for tension mode under thermal load by DMA

- GF DiCoFRTS

Resin system	VE resin
Fiber type	Glass
Fiber length	25 mm
Fiber content	41 wt.-%, 23 vol.-%

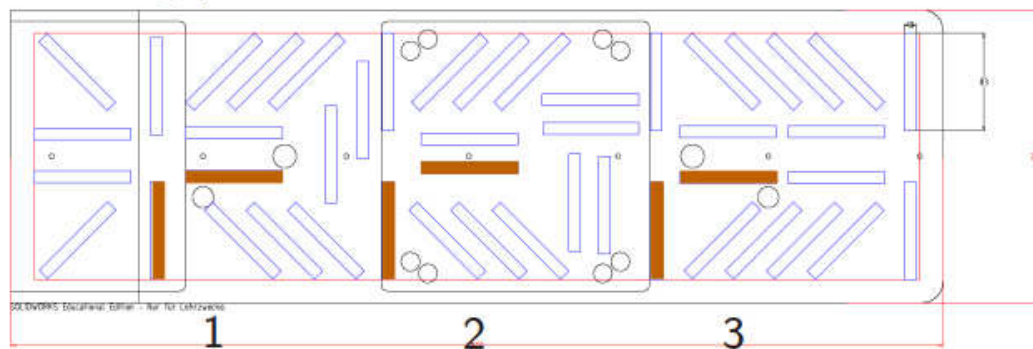


- Plate specifications:

800 mm × 250 mm × 2 mm

- Filling of plate with resin at 33%, 50% and 100%

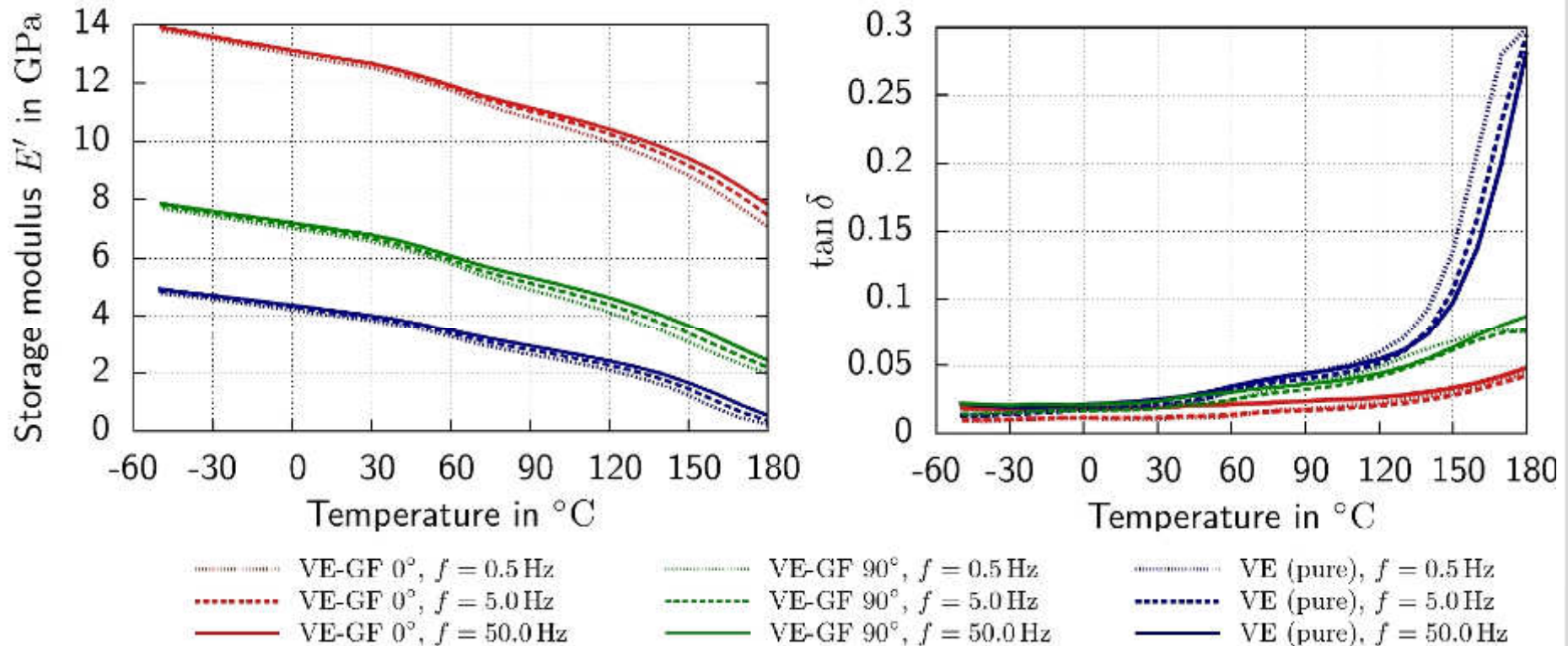
- Cutting plan



Mould charged with approx.
60% of semi-finished product

Experimental results for tension mode under thermal load by DMA

- Comparison of storage modulus for different temperature and frequency loads on VE-GF and pure VE



- Test parameters:

Static load $\varepsilon_{\text{stat}} = 0.1\%$

Dynamic load $\varepsilon_{\text{dyn}} = 0.05\%$

Contact force $F_c = 5 \text{ N}$

Load cell capacity 500 N

Hashin-Shtrikman related two-step method

Walpole (9169), Willis (1977), Willis(1981), Müller (2015)

- Based on generalized formulation with eigenstrains
 - First step

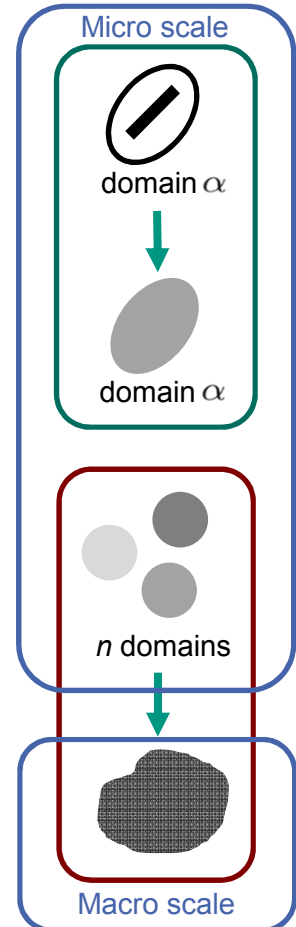
$$\bar{\mathbb{C}}_{\alpha}^{\text{UD+}} = \mathbb{C}_{\alpha} + c_M (\mathbb{C}_M - \mathbb{C}_{\alpha}) \left(\mathbb{I}^S + c_{\alpha} \mathbb{P}_{\alpha}^{\text{UD}} (\mathbb{C}_M - \mathbb{C}_{\alpha}) \right)^{-1}$$

$$\bar{\mathbb{C}}_{\alpha}^{\text{UD-}} = \mathbb{C}_M + c_{\alpha} (\mathbb{C}_{\alpha} - \mathbb{C}_M) \left(\mathbb{I}^S + c_M \mathbb{P}_{\alpha}^{\text{UD}} (\mathbb{C}_{\alpha} - \mathbb{C}_M) \right)^{-1}$$

- Second step

$$\bar{\mathbb{C}}^{\text{HS}\pm} = \sum_{\alpha=1}^n \frac{c_{\alpha}}{c_F} \bar{\mathbb{C}}_{\alpha}^{\text{UD}\pm} \mathbb{A}_{\alpha}^{\text{HS}} = \sum_{\alpha=1}^n \frac{c_{\alpha}}{c_F} \bar{\mathbb{C}}_{\alpha}^{\text{UD}\pm} \mathbb{M}_{\alpha} \langle \mathbb{M} \rangle^{-1}$$

$$\mathbb{M}_{\alpha} = \left(\mathbb{I}^S + \mathbb{P}_0 (\bar{\mathbb{C}}_{\alpha}^{\text{UD}\pm} - \mathbb{C}_0) \right)^{-1} \quad \text{and} \quad \langle \mathbb{M} \rangle = \sum_{\alpha=1}^n \frac{c_{\alpha}}{c_F} \mathbb{M}_{\alpha}$$



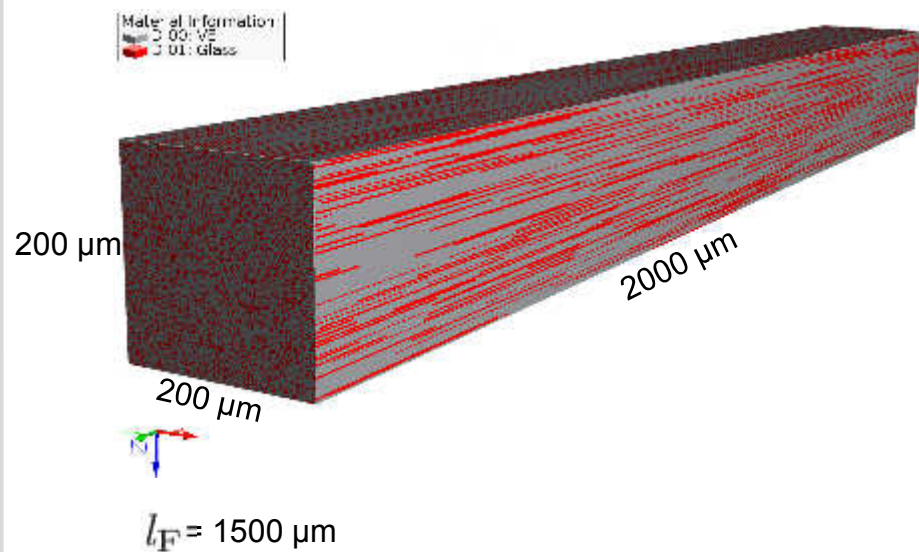
- Two-step method for formulation with variable reference stiffness \mathbb{C}_0

$$\mathbb{C}_0 = (1 - a) \mathbb{C}_M + a \mathbb{C}_F \quad a \in [0, 1]$$

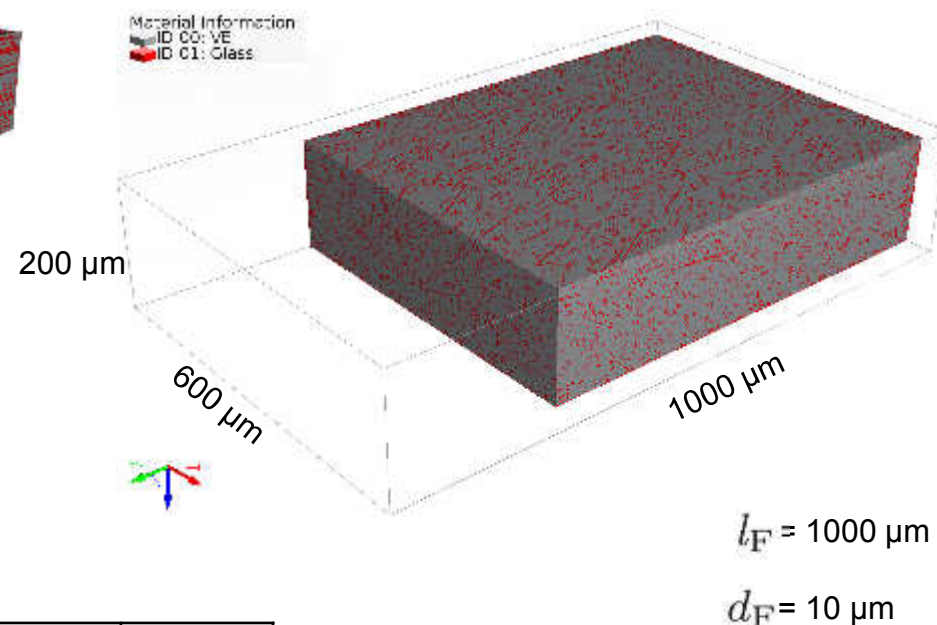
Mean field and full field simulation

- Virtual microstructure generated with GeoDict®

- Unidirectional long fibers



- Randomly non-uniform distributed long fibers

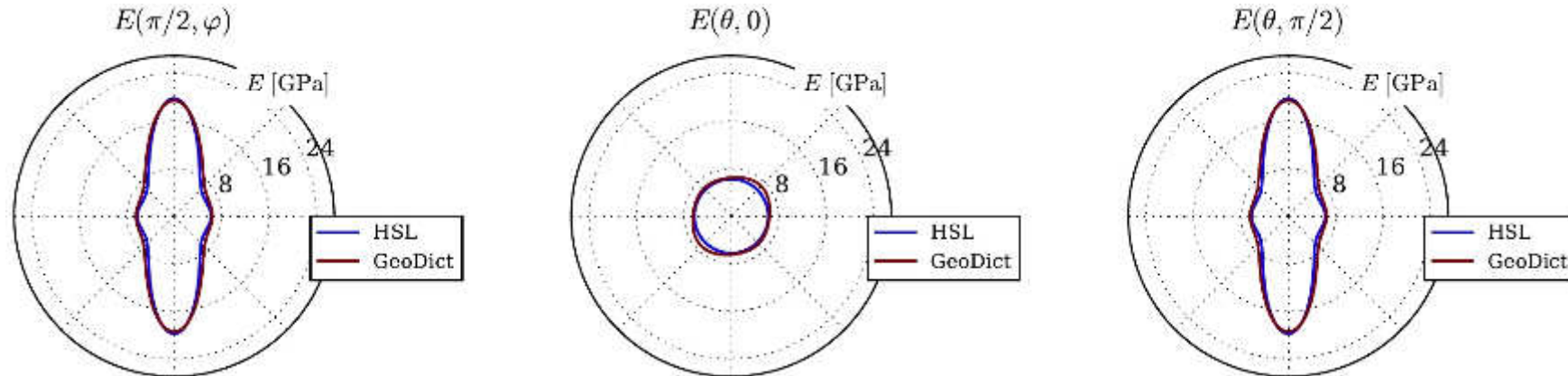


- Material parameters:

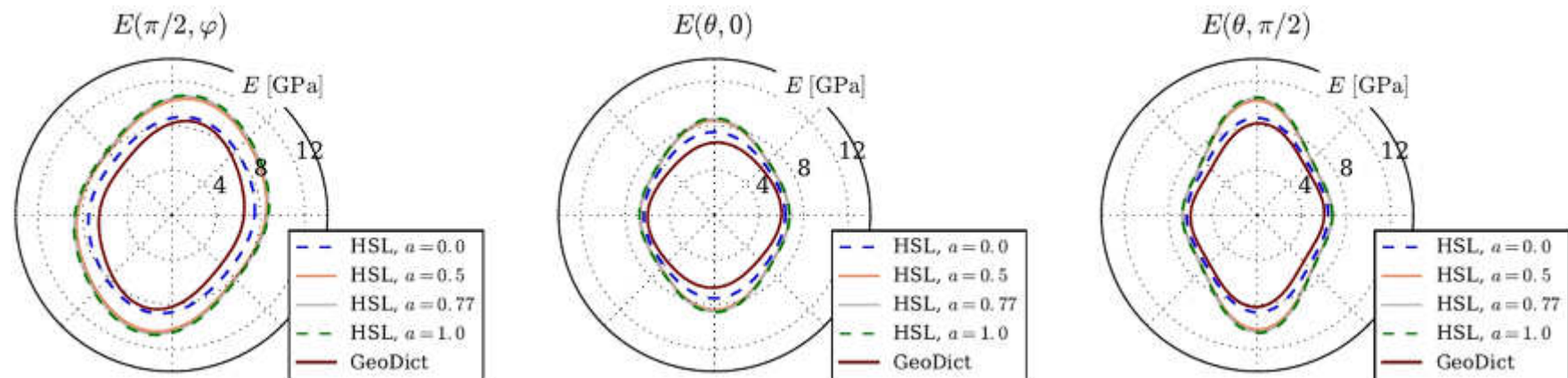
Matrix	Young's modulus E_M	4.0 MPa
Fiber	Poisson's ratio ν_M	0.35
Matrix	Young's modulus E_F	73.0 MPa
Fiber	Poisson's ratio ν_F	0.22
Fiber	Fiber volume fraction c_F	0.23

Comparison between full field and mean field homogenization

■ Young's modulus for UD fibers in matrix material



■ Young's modulus for randomly non-uniform distributed fibers in matrix material



Macroscale Simulation and Characterization

Contact:

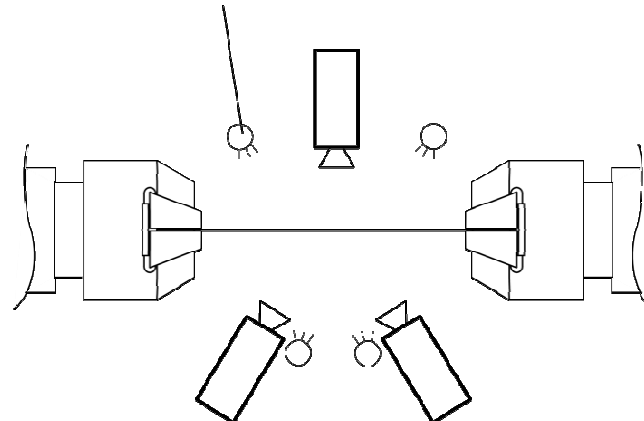
Malte Schemmann, malte.schemmann@kit.edu, KIT ITM

Biaxial Tensile Machine (ITM)



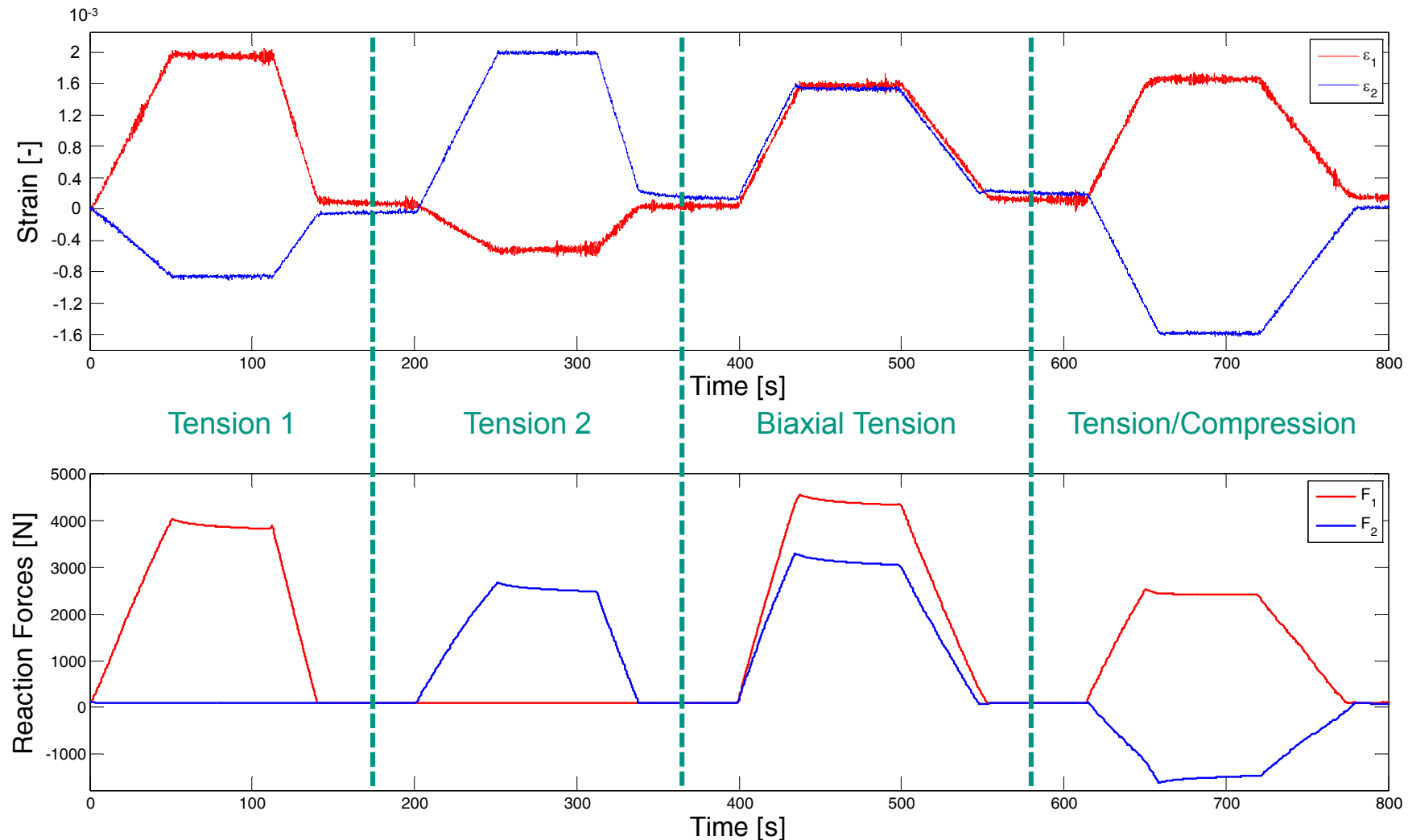
- Actors: four independent axes (maximum load: 150kN)
- Sensors:
 - Force measurement (on all four axes)
 - Integrated strain (Video XTens)
 - Full strain field via digital image correlation (GOM ARAMIS 4M)
- Active midpoint control

Video XTens
Specimen lighting

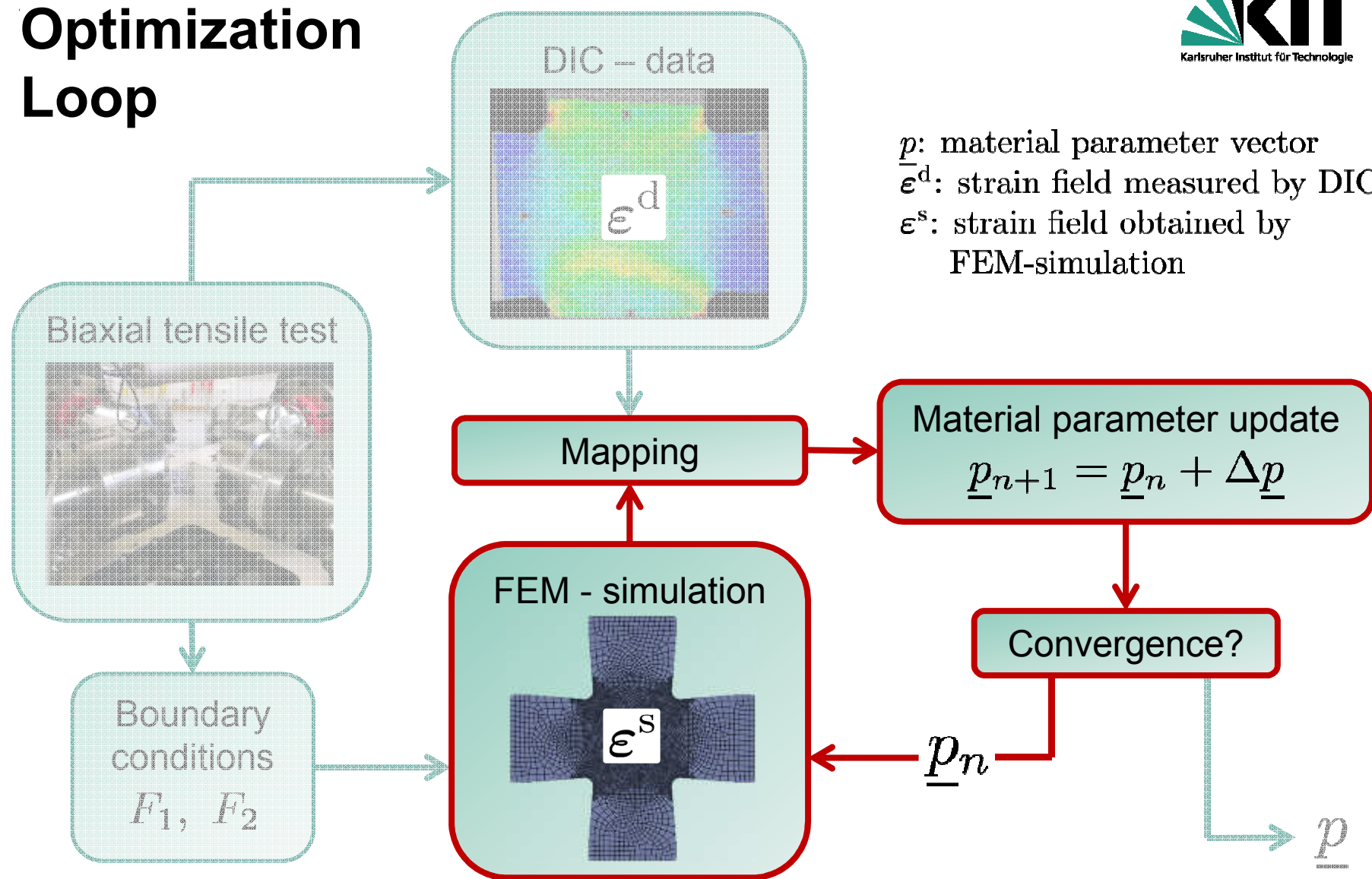


ARAMIS

Viscoelastic Biaxial Tensile Tests: Prescribed Strain / Force Paths



Optimization Loop



Inverse Parameter Identification

- Problem: Find parameter \underline{p} that minimizes the error Function $f(\underline{p})$

$$\underline{r}(\underline{p}) = \sum_{i=1}^K \sum_{j=1}^N \begin{pmatrix} |\varepsilon_{11,i,j}^{\text{sim}}(\underline{p}) - \varepsilon_{11,i,j}^{\text{exp}}| \\ |\varepsilon_{22,i,j}^{\text{sim}}(\underline{p}) - \varepsilon_{22,i,j}^{\text{exp}}| \\ |\gamma_{12,i,j}^{\text{sim}}(\underline{p}) - \gamma_{12,i,j}^{\text{exp}}| \end{pmatrix}$$

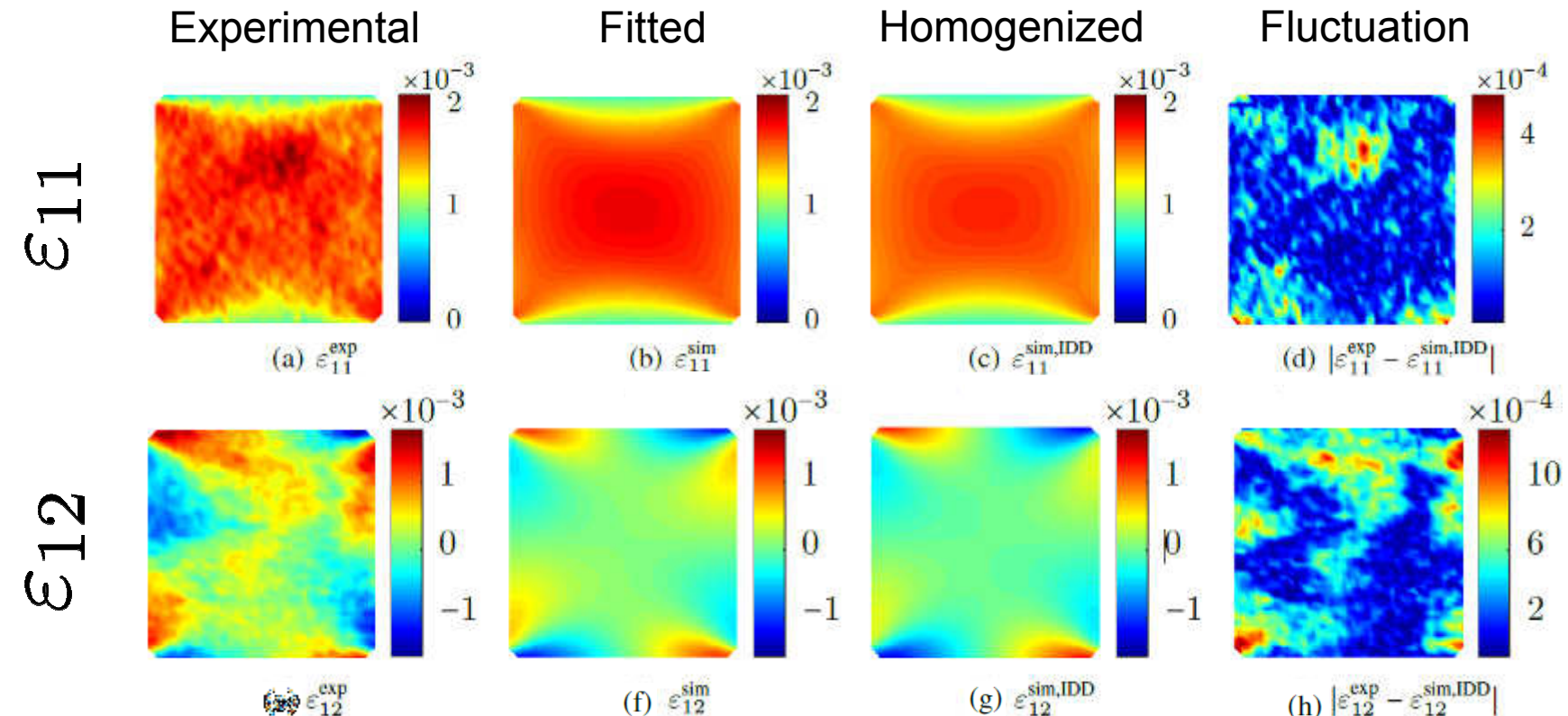
Louis (1989)
Mahnken et al. (1996)
Cooreman et al. (2007)

- Gauss-Newton procedure

$$f(\underline{p}) = \|\underline{r}(\underline{p})\|_2^2 = \underline{r}(\underline{p})^\top \underline{r}(\underline{p}) \rightarrow \min_{\underline{p} \in \mathcal{P}}$$

$$\underline{p}^{k+1} = \underline{p}^k - [\underline{\underline{J}}(\underline{p}^k)^\top \underline{\underline{J}}(\underline{p}^k)]^{-1} \underline{\underline{J}}(\underline{p}^k)^\top \underline{r}(\underline{p}^k) \quad J_{ij}(\underline{p}) = \frac{\partial \varepsilon_i^s(\underline{p})}{\partial p_j}$$

Validation Tension-Compression Loading



- The experimentally measured, fitted and homogenized strain field show a comparably good agreement
- SMC shows heterogeneities, possibly induced by varying fiber orientation or volume fraction

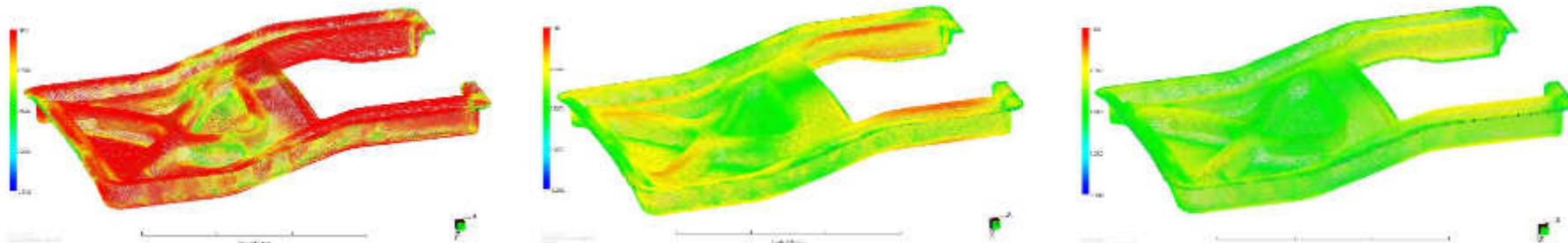
[Contact: Malte Schemmann, malte.schemmann@kit.edu, Loredana Kehrer, loredana.kehrer@kit.edu, KIT ITM]

Form Filling: Micromechanical Modeling

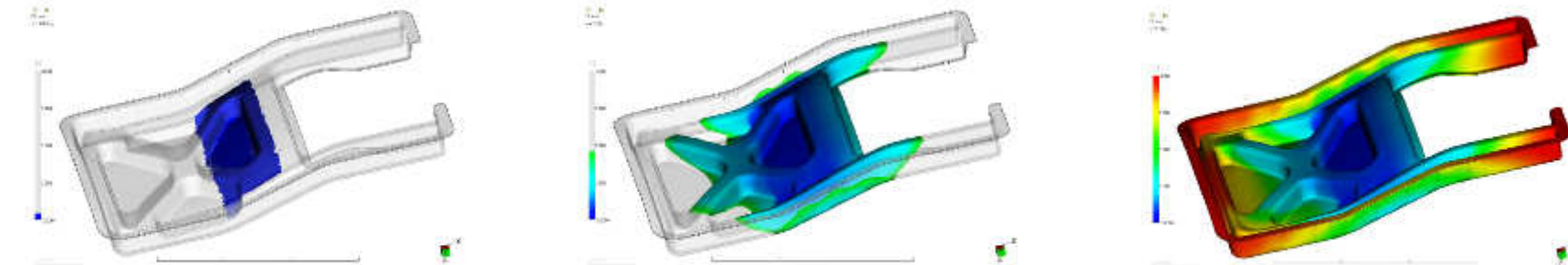
Contact: Robert Bertoti, robert.bertoti@kit.edu, KIT ITM

Form Filling Simulations – Motivation

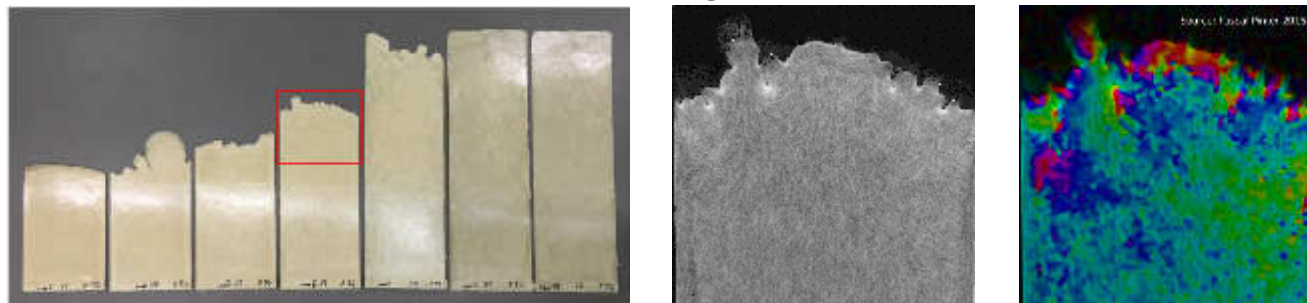
- Prediction of the **fiber orientation** of compression molded DiCoFRP (Buck2014)



- Prediction of the **flow front evolution** during compression molding (Buck2014)



- Development of the simulations through **comparison to experiments**



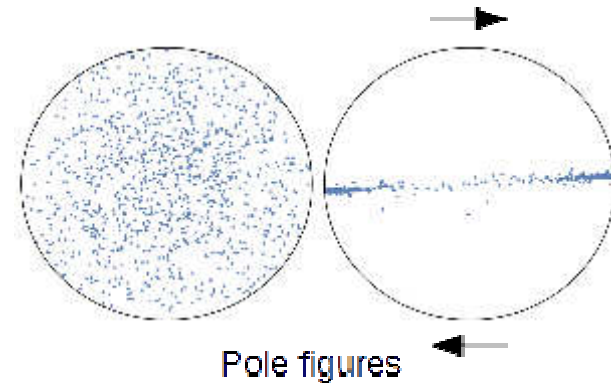
Evolution equations of Single Fiber and FOTs

- Change of single rigid-fiber orientation (Jeffery1922)

$$\dot{\mathbf{n}}_\alpha = \bar{\mathbf{W}}[\mathbf{n}_\alpha] + \bar{\xi}(\bar{\mathbf{D}}[\mathbf{n}_\alpha] - (\mathbf{n}_\alpha \otimes \mathbf{n}_\alpha \otimes \mathbf{n}_\alpha)[\bar{\mathbf{D}}])$$

where: $\bar{\mathbf{L}} = \text{grad}(\bar{\mathbf{v}}) = \bar{\mathbf{D}} + \bar{\mathbf{W}}$ $\bar{\mathbf{D}} = \frac{1}{2}(\bar{\mathbf{L}} + \bar{\mathbf{L}}^T)$

$$\bar{\mathbf{W}} = \frac{1}{2}(\bar{\mathbf{L}} - \bar{\mathbf{L}}^T) \quad \bar{\xi} = \frac{\bar{a}^2 - 1}{\bar{a}^2 + 1} \quad \bar{a} = \bar{l}/\bar{d}$$

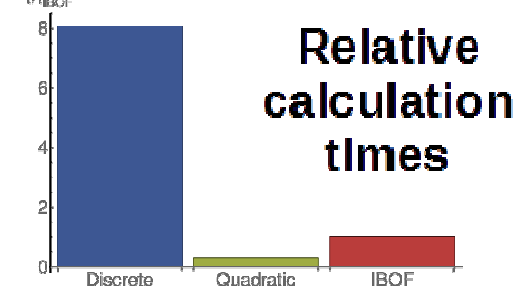
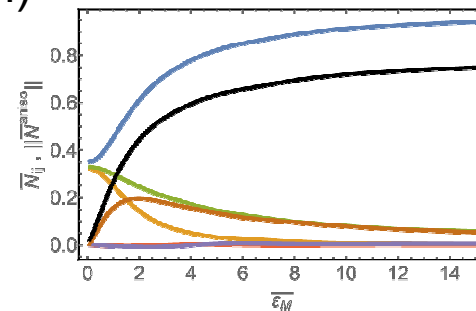


- Jeffery's equation for FOTs (including closure problem)

$$\dot{\bar{\mathbf{N}}} = \bar{\mathbf{W}}\bar{\mathbf{N}} - \bar{\mathbf{N}}\bar{\mathbf{W}} + \bar{\xi}(\bar{\mathbf{D}}\bar{\mathbf{N}} + \bar{\mathbf{N}}\bar{\mathbf{D}} - 2\bar{\mathbf{N}}^*[\bar{\mathbf{D}}])$$

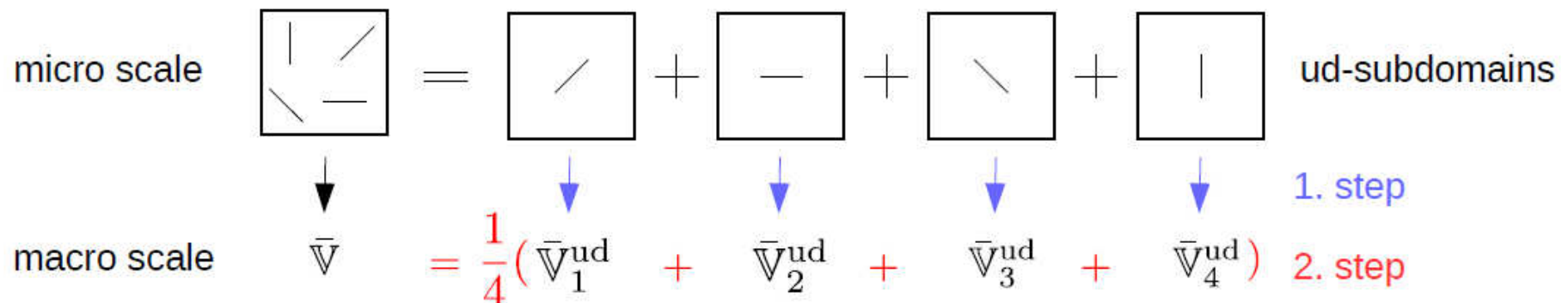
where: $\bar{\mathbf{N}}^{\text{Quad}} = \bar{\mathbf{N}} \otimes \bar{\mathbf{N}}$ (Doi1981)

$$\begin{aligned} \bar{\mathbf{N}}^{\text{IBOF}} &= \beta_1 \text{ sym}(\mathbf{1} \otimes \mathbf{1}) + \\ &\quad \beta_2 \text{ sym}(\mathbf{1} \otimes \bar{\mathbf{N}}) + \\ (\text{Chung2002}) \quad &\quad \beta_3 \text{ sym}(\bar{\mathbf{N}} \otimes \bar{\mathbf{N}}) + \\ &\quad \beta_4 \text{ sym}(\mathbf{1} \otimes \bar{\mathbf{N}}\bar{\mathbf{N}}) + \\ &\quad \beta_5 \text{ sym}(\bar{\mathbf{N}} \otimes \bar{\mathbf{N}}\bar{\mathbf{N}}) + \\ &\quad \beta_6 \text{ sym}(\bar{\mathbf{N}}\bar{\mathbf{N}} \otimes \bar{\mathbf{N}}\bar{\mathbf{N}}) \end{aligned}$$



Relative
calculation
times

Homogenization of the viscosity



- 1. step: calculating the unidirectional effective viscosity(s) (Hasin-Strikman lower bound) (Walpole1969, Castaneda1998)
- 2. step: calculating the overall effective linear viscosity (orientation averaging, Voigt average, upper bound) (Advani1987)
- It is sufficient to calculate the unidirectional effective viscosity only once, and calculate the overall effective viscosity with the help of FOTs

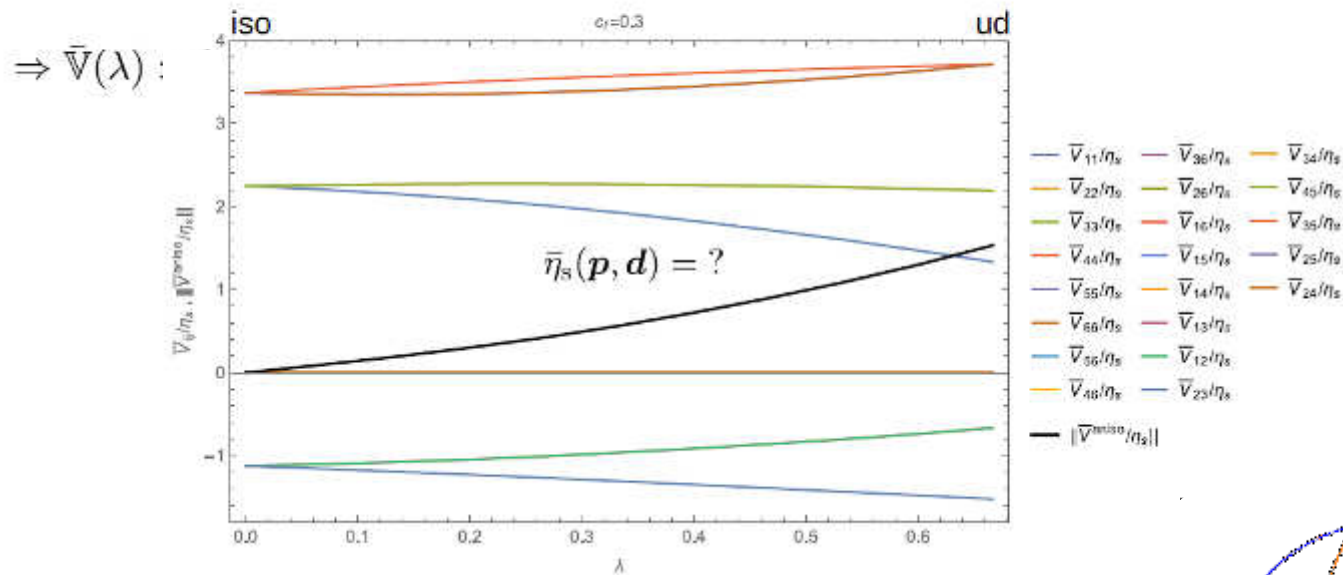
$$\bar{\mathbb{V}}_{\alpha}^{\text{ud}} = \mathbb{V}^m + \frac{c_f}{c_m} \mathbb{P}_{\alpha}^{-1}$$

$$\bar{\mathbb{V}} = \frac{1}{N} \sum_{\alpha=1}^N \bar{\mathbb{V}}_{\alpha}^{\text{ud}}$$

$$\bar{\mathbb{V}} = f(\bar{\mathbb{V}}_x^{\text{ud}}, \bar{\mathbf{N}}, \bar{\mathbb{N}})$$

Homogenization of the viscosity

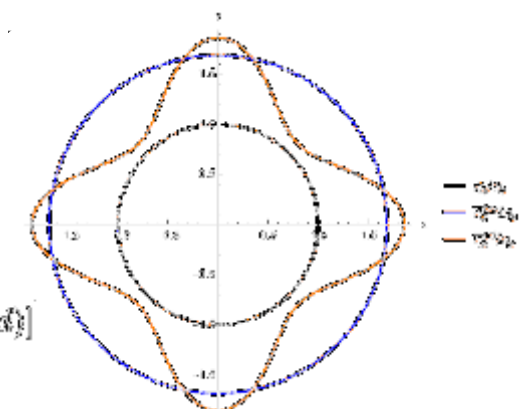
$$\bar{\mathbf{N}}^{\text{iso}}(\lambda = 0) = \begin{pmatrix} \frac{1}{3} & & \\ & \frac{1}{3} & \\ & & \frac{1}{3} \end{pmatrix} \quad \bar{\mathbf{N}}(\lambda) = \begin{pmatrix} \frac{1}{3} + \lambda & & \\ & \frac{1}{3} + \frac{\lambda}{2} & \\ & & \frac{1}{3} + \frac{\lambda}{2} \end{pmatrix} \quad \bar{\mathbf{N}}^{\text{ud}}(\lambda = \frac{2}{3}) = \begin{pmatrix} 1 & 0 & 0 \end{pmatrix}$$



Sensitivity of the effective tensorial viscosity

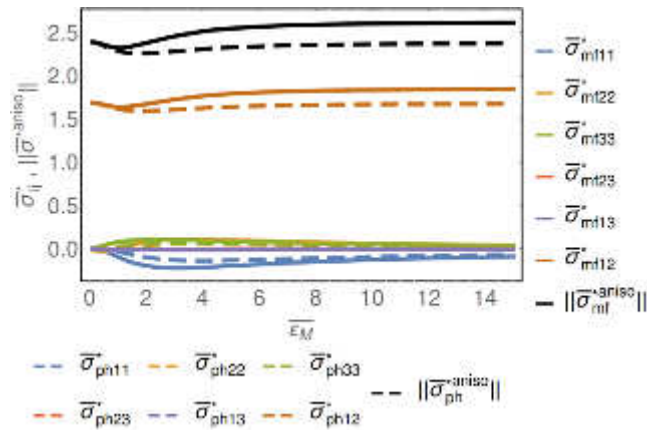
$$\tilde{\eta}_s(p, d) = \frac{1}{2M(p, d) \cdot \bar{V}^{-1} [M(p, d)]}$$

$$M(p, d) = \sqrt{2}(p \otimes d + d \otimes p)/2$$

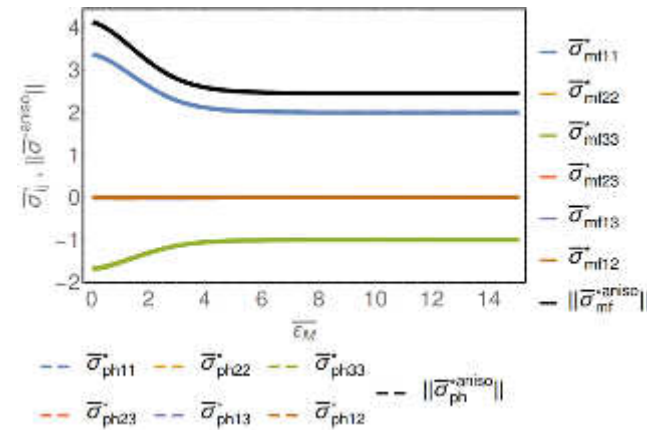


Test Cases – Stress tensor

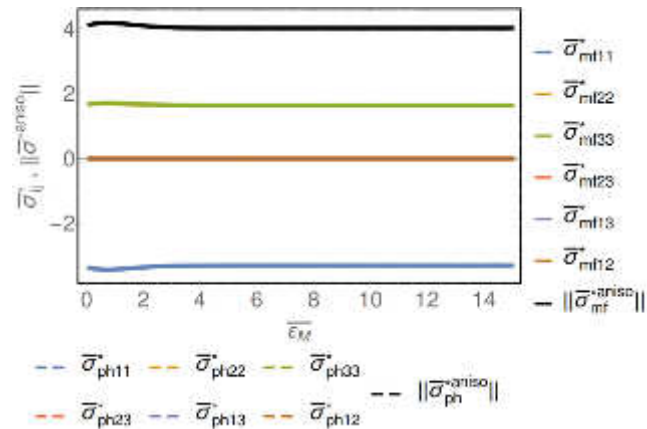
Simple shear flow



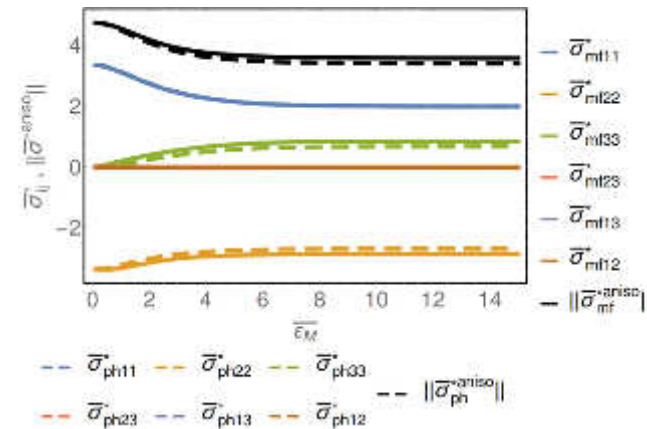
Isochoric elongation flow



Isochoric compression flow



Plain strain flow



Conclusions and Outlook

- An **interdisciplinary and integrated engineering** approach is necessary for the application of CoDiCoFRP
- A virtual process chain is required for taking the highly process-dependent material properties into account
- Adaption and validation of a complex virtual process chain is only feasible with a **standardization data formats**
- Future work will extend the material range the thermoplastics
- A reference structure will be established by GRK 2078 in 2017 :
 - Incorporation of all technology projects within the process chain
 - Geometry is obtained by fully coupled design optimization, thereby considering modfilling and structural analysis including damage

Thank you for your attention.

The research documented in this manuscript has been funded by the German Research Foundation (DFG) within the International Research Training Group “**Integrated engineering of continuous-discontinuous long fiber-reinforced polymer structures**” (GRK 2078).

The support by the German Research Foundation (DFG) is gratefully acknowledged.

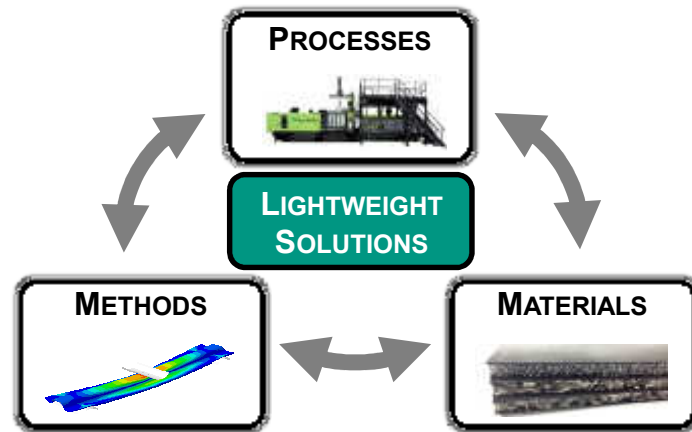


GRK 2078 CoDiCoFRP

www.grk2078.kit.edu



KIT - LIGHTWEIGHT DESIGN NETWORK



www.leichtbau.kit.edu

Contact

thomas.boehlke@kit.edu
Karlsruhe Institute of Technology (KIT)
Institute of Engineering Mechanics (ITM)
Chair for Continuum Mechanics

